Proceedings of the ASME 2012 31st International Conference on Ocean, Offshore and Arctic Engineering
OMAE2012
July 1-6, 2012, Rio de Janeiro, Brazil

OMAE2012-83294

DISTRIBUTED WAKE-BODY RESONANCE OF A LONG FLEXIBLE CYLINDER IN SHEAR FLOW

Rémi Bourguet*
Institut de Mécanique des Fluides de Toulouse
Toulouse, France
Email: bourguet@imft.fr

Michael S. Triantafyllou
Massachusetts Institute of Technology
Cambridge, MA, USA
Email: mistetri@mit.edu

Michael Tognarelli
BP America Production Co.
Houston, TX, USA
Email: michael.tognarelli@bp.com

Pierre Beynet
BP America Production Co.
Houston, TX, USA
Email: pierre.beynet@bp.com

ABSTRACT

The fluid-structure interaction mechanisms involved in the development of narrowband and broadband vortex-induced vibrations of long flexible structures placed in non-uniform currents are investigated by means of direct numerical simulation. We consider a tensioned beam of aspect ratio 200*, free to move in both the in-line and cross-flow directions, and immersed in a sheared flow at Reynolds number* 330*. Both narrowband and broadband multi-frequency vibrations may develop, depending on the velocity profile of the sheared oncoming current.*

Narrowband vibrations occur when lock-in, i.e. the synchronization between vortex shedding and structure oscillations, is limited to a single location along the span, within the high current velocity region; thus, well-defined lock-in versus non-lock-in regions are noted along the span. In contrast, we show that broadband responses, where both high and low structural wavelengths are excited, are characterized by several isolated regions of lock-in, distributed along the length. The phenomenon of distributed lock-in impacts the synchronization of the in-line and cross-flow vibrations, and the properties of the fluid-structure energy transfer, as function of time and space.

*Address all correspondence to this author.

INTRODUCTION

Vortex shedding in the wake of a riser or cable subject to a cross-flow current induces unsteady fluid forces on the structure, resulting in structural vibrations and stresses that can cause fatigue damage.

The case of a rigid circular cylinder free to move, or forced to oscillate within a uniform current, has served as a canonical problem to investigate VIV mechanisms (Bearman, 1984; Ongoren & Rockwell, 1988; Sarpkaya, 2004; Williamson & Govardhan, 2004; Carberry *et al.*, 2005; Prasanth & Mittal, 2008; Bearman, 2011). Large amplitude oscillations occur when the frequency of vortex formation is relatively close to a natural frequency of the structure; then the frequency of vortex shedding can be entrained and become equal to the frequency of the structural vibration. This condition of wake-body resonance is referred to as *lock-in*.

The increased complexity of the VIV phenomenon in the case of slender flexible bodies immersed in sheared currents, has been highlighted in recent experimental and numerical works (Trim *et al.*, 2005; Lie & Kaasen, 2006; Lucor *et al.*, 2006; Vandiver *et al.*, 2009; Bourguet *et al.*, 2011*a*). Mono-frequency as well as multi-frequency structural responses have been reported in this context (Chaplin *et al.*, 2005; Bourguet *et al.*, 2011*b*). The occurrence of multi-frequency vibrations may significantly im-

pact the fatigue life of the structures. However, previous studies were limited to narrowband vibrations and the case of broadband responses, where both high and low structural wavenumbers are excited, still remains to be investigated.

We address this problem of broadband response using detailed numerical simulation results. The objective is to analyze the fluid-structure interaction mechanisms associated with broadband VIV in non-uniform current, with an emphasis on the lock-in phenomenon and its impact on the energy transfer between the flow and the body.

The physical model and numerical method are briefly described in a first section. The structural vibrations are analyzed in a second section. Lock-in and fluid-structure energy transfer are examined in a third section. The main findings of this study are summarized in a fourth section.

PHYSICAL MODEL AND NUMERICAL METHOD

The flow past a flexible cylinder of circular cross-section is predicted using direct numerical simulation of the three-dimensional incompressible Navier-Stokes equations. The cylinder is submitted to a cross-flow which is parallel to the global x axis and sheared along the global z axis. Two types of sheared profiles, linear and exponential, are used as shown in Fig. 1. In both cases, the ratio between the maximum and minimum oncoming flow velocities is set to 3.67. In the following, all physical variables are non-dimensionalized using the cylinder diameter D and the maximum inflow velocity U, which occurs at $z = 0$. The Reynolds number (Re) based on D and U is equal to 330.

The cylinder aspect ratio is $L/D = 200$, where L is the cylinder length in its equilibrium position in quiescent fluid. It is pinned at both ends, while it is free to move in both the in-line (x) and cross-flow (y) directions. The cylinder mass ratio, defined as $m = \rho_c/\rho_f D^2$, where ρ_c is the cylinder mass per unit length and ρ_f the fluid density, is set to 6. The constant tension, bending stiffness and damping of the structure are designated by T, EI and K, respectively. The in-line and cross-flow displacements of the cylinder are denoted by ζ_x and ζ_y. The sectional drag and lift coefficients are defined as $C_x = 2F_x/\rho_f DU^2$ and $C_y = 2F_y/\rho_f DU^2$, where F_x and F_y are the in-line and cross-flow dimensional fluid forces. The structural dynamics are governed by a tensioned beam model, expressed as follows in non-dimensional form (Evangelinos & Karniadakis, 1999):

$$\frac{\partial^2 \zeta}{\partial t^2} - \omega_c^2 \frac{\partial^2 \zeta}{\partial z^2} + \omega_b^2 \frac{\partial^4 \zeta}{\partial z^4} + \frac{K}{m}\frac{\partial \zeta}{\partial t} = \frac{1}{2}\frac{C}{m}, \qquad (1)$$

where $\zeta = [\zeta_x, \zeta_y]^T$ and $C = [C_x, C_y]^T$. t denotes the non-dimensional time variable. ω_c and ω_b, the cable and beam phase velocities defined as $\omega_c^2 = T/m$ and $\omega_b^2 = EI/m$, are set to similar values in both cases, $(\omega_c, \omega_b) = (4.55, 9.09)$ in the linear profile case and $(\omega_c, \omega_b) = (5, 10)$ in the exponential profile case. The structural damping is set equal to zero ($K = 0$) to allow maximum amplitude oscillations. These structural parameters lead to vibrations involving high structural wavenumbers, which are representative of configurations encountered in the context of ocean engineering (Trim *et al.*, 2005).

The parallelized code *Nektar*, based on the spectral/*hp* element method (Karniadakis & Sherwin, 1999), is used to solve the coupled fluid-structure system. A boundary-fitted coordinate formulation is used to take into account the cylinder unsteady deformation. The version of the code employs a hybrid scheme with Fourier expansion in the spanwise (z) direction and Jacobi-Galerkin formulation in the (x,y) planes. Validation studies of the numerical method have been reported in previous works concerning similar physical configurations (Newman & Karniadakis, 1997; Evangelinos & Karniadakis, 1999; Bourguet *et al.*, 2011*a*). The present simulations involve approximately 0.6×10^9 degrees of freedom. The results reported in this study are based on time series of more than 300 convective time units, collected after the initial transient dies out.

NARROWBAND VERSUS BROADBAND MULTI-FREQUENCY RESPONSES

The typical structural vibrations observed in the cases of linear and exponential shear profiles are illustrated in Fig. 2(a) and (b), respectively. Selected time series of the cylinder cross-flow displacement are presented. In both cases, the response is a mixture of standing and traveling wave patterns. The amplitude of oscillation in the case of exponential shear is approximately half the amplitude observed in the linear shear case, in both the in-line and cross-flow directions (Fig. 3). In these plots, only the deviations of the in-line motion from its mean value, $\tilde{\zeta}_x$, are considered. In the case of linear shear, the underlying standing wave component leads to the formation of cells along the span corresponding to alternating 'nodes' (minima of the response envelope) and 'anti-nodes' (maxima of the response envelope). Such cellular patterns are not observed in the exponential shear case, due to a change in the nature of the responses, as shown in the following.

The response power spectral densities (PSD) are plotted in Fig. 4. Both cases exhibit multi-frequency vibrations but the structural responses differ by the excited frequency bandwidth and the range of excited wavenumbers: three main frequencies are excited along the span within a narrow band in the case of linear shear while a broadband response is observed in the exponential shear case. Through spatio-temporal spectral analysis, each excited frequency can be related to the corresponding excited structural wavenumber. In the case of narrowband response, only high wavenumbers, corresponding to three adjacent sine Fourier modes, are excited. In the case of broadband vibrations, both high- and low-wavenumber responses are noted. The

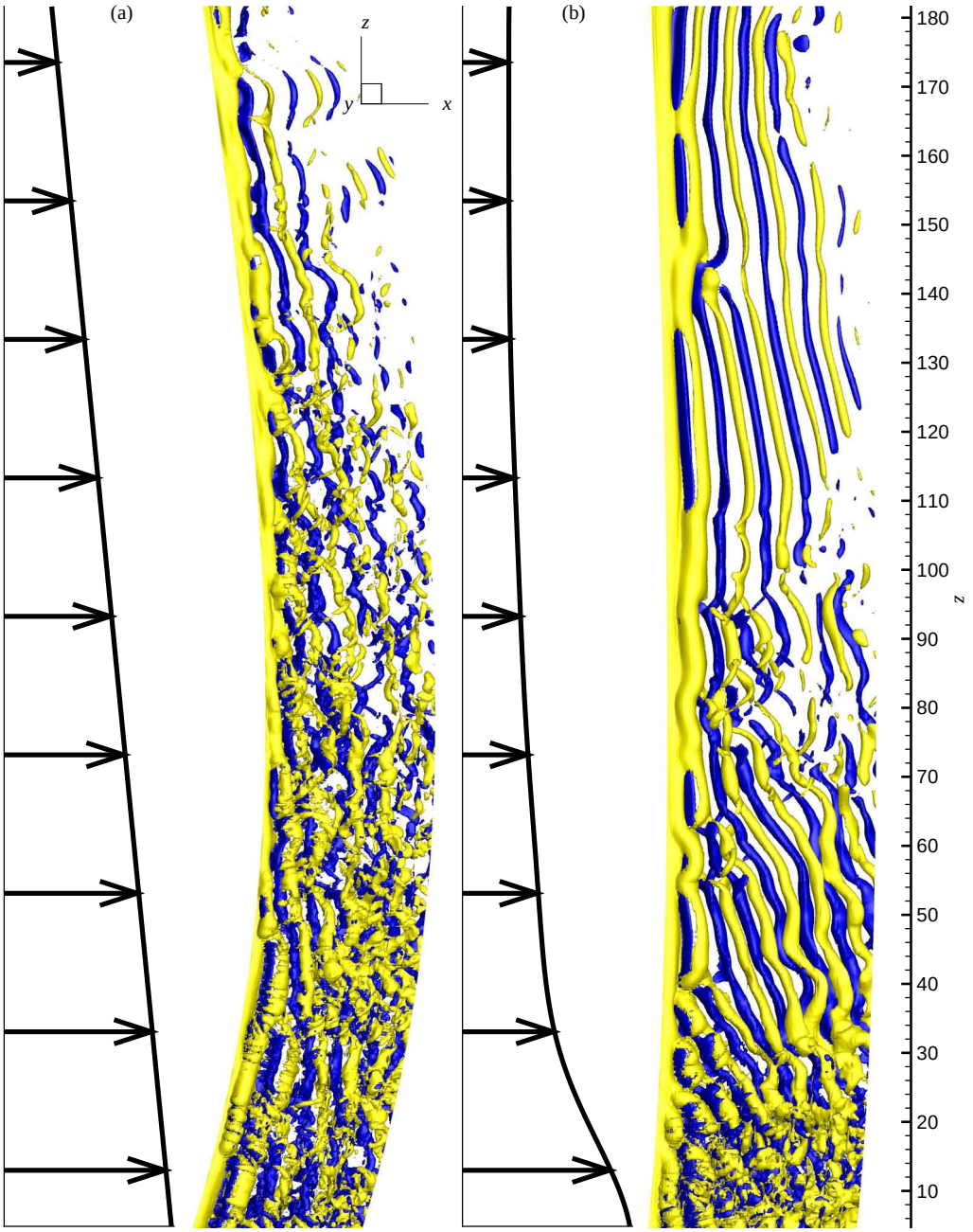

FIGURE 1. INSTANTANEOUS ISO-SURFACES OF SPANWISE VORTICITY DOWNSTREAM OF THE CYLINDER: (a) LINEAR VELOCITY PROFILE ($\omega_z = \pm 0.3$) AND (b) EXPONENTIAL VELOCITY PROFILE ($\omega_z = \pm 0.15$). PART OF THE COMPUTATIONAL DOMAIN IS SHOWN. ARROWS REPRESENT THE SHEAR ONCOMING FLOW.

in-line responses also exhibit a clear narrowband or broadband character, depending on the oncoming flow velocity profile.

The in-line and cross-flow vibrations are non-linearly coupled by the fluid forces. The phase difference between the in-line and cross-flow displacements controls the shape and orientation of the beam trajectories in the plane perpendicular to the span. The instantaneous phases of the in-line and cross-flow displacements (ϕ_x and ϕ_y respectively) are determined by means of the Hilbert transform. Adopting an approach similar to Huera-Huarte & Bearman (2009), the phase difference Φ_{xy} is quantified

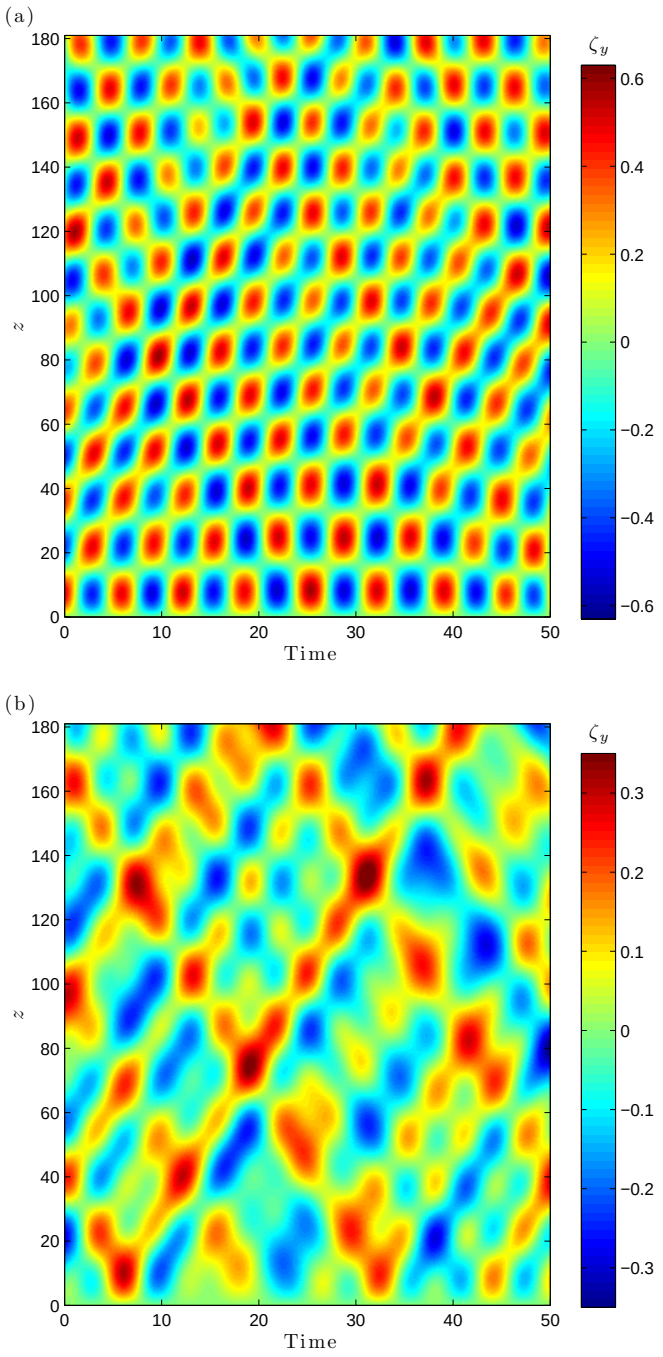

FIGURE 2. TEMPORAL EVOLUTION OF CROSS-FLOW DISPLACEMENT ALONG THE CYLINDER SPAN, IN THE CASES OF (a) LINEAR AND (b) EXPONENTIAL VELOCITY PROFILES.

as follows:

$$\Phi_{xy} = [p\phi_x - q\phi_y, \quad \mod 360^o], \tag{2}$$

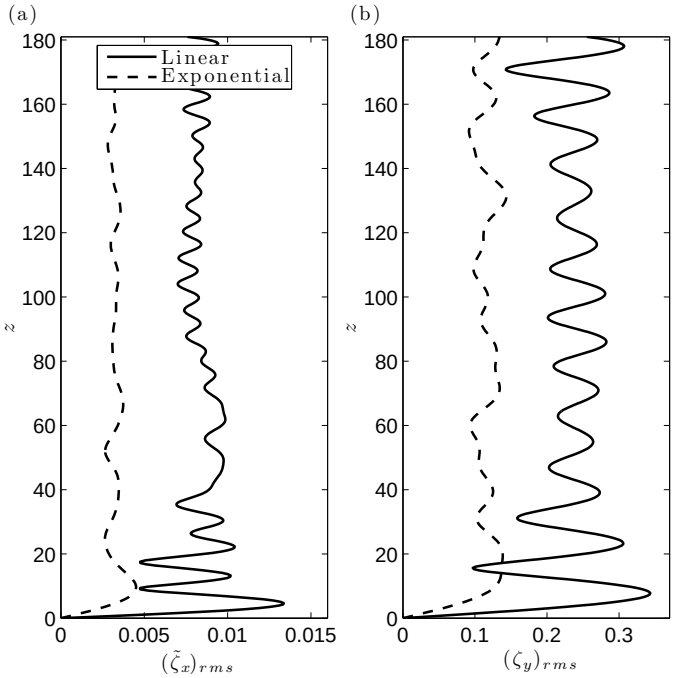

FIGURE 3. RMS VALUE OF (a) IN-LINE DISPLACEMENT FLUCTUATION AND (b) CROSS-FLOW DISPLACEMENT ALONG THE CYLINDER SPAN.

where p and q are two integer numbers defining the level of synchronization studied. As generally observed in this context, a ratio of 2 can be established between in-line and cross-flow excited frequencies; hence the couple $(p,q) = (1,2)$ is chosen here. Values of Φ_{xy} in the range $0^o - 180^o$ ($180^o - 360^o$ respectively) correspond to 'figure eight' orbits, where the beam moves upstream (downstream respectively) when reaching the cross-flow oscillation maxima. These two types of trajectories are referred to as 'counter-clockwise' and 'clockwise', respectively (Dahl *et al.*, 2007).

The histograms of Φ_{xy} issued from the entire response time series are plotted along the span in Fig. 5, for both velocity profiles. In the linear shear case, a predominant trajectory can be identified at each spanwise location (Fig. 5(a)). In this case, due to the pronounced standing wave character of the vibrations near $z = 0$, transitions can be noted between counter-clockwise and clockwise trajectories near the nodes of the in-line response. In the region where purer traveling waves develop, the phase difference exhibits a well-defined, nearly-linear drift towards higher angles, as z increases. Counter-clockwise orbits dominate the synchronization pattern in the high velocity region. Significant differences can be noted in the case of broadband responses (Fig. 5(b)). Despite noisier histograms, it appears that Φ_{xy} remains generally lower than 180^o; hence, the in-line and cross-flow vibrations appear to be locked to a specific phase difference

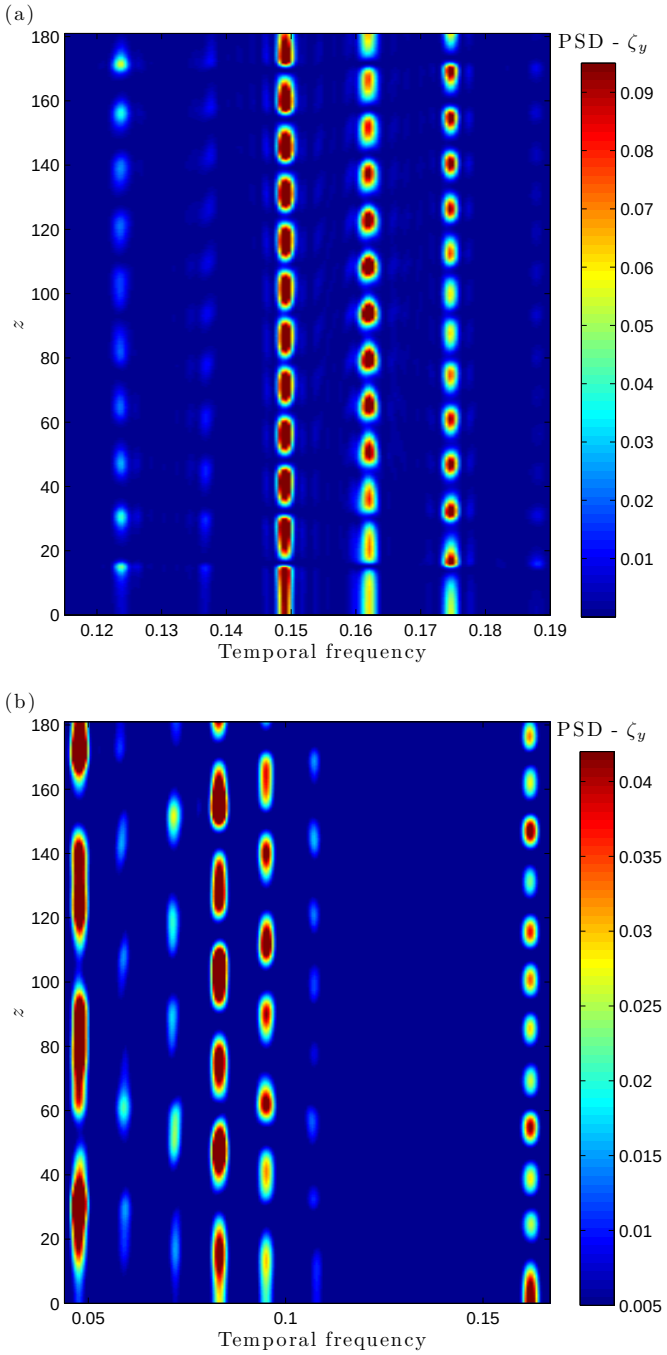

FIGURE 4. SPANWISE EVOLUTION OF CROSS-FLOW DISPLACEMENT PSD, IN THE CASES OF (a) LINEAR AND (b) EXPONENTIAL VELOCITY PROFILES.

range and no drift can be identified along the beam.

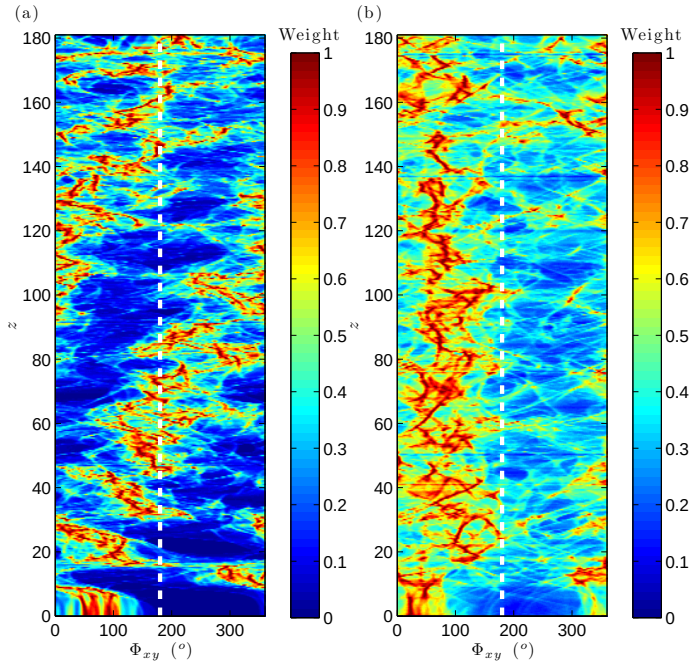

FIGURE 5. HISTOGRAM OF IN-LINE/CROSS-FLOW MOTION PHASE DIFFERENCE ALONG THE CYLINDER SPAN, IN THE CASES OF (a) LINEAR AND (b) EXPONENTIAL VELOCITY PROFILES.

DISTRIBUTED LOCK-IN AND FLUID-STRUCTURE ENERGY TRANSFER

For long flexible structures, the lock-in condition is defined to exist at each spanwise location where the local vortex shedding frequency is synchronized with a cross-flow vibration frequency; otherwise, the condition is referred to as non-lock-in. A spanwise region which envelopes all the adjacent locked-in locations is referred to as a lock-in region. The PSD of the cross-flow component of the flow velocity in the wake is used to identify the vortex shedding frequency along the span (Fig. 6).

In the case of linear shear (narrowband responses), a single lock-in region is found, located within the high current velocity, while over the rest of the span vortex shedding and cylinder vibrations are not synchronized.

In contrast, the case of exponential shear (broadband responses) exhibits a totally different behavior: the lock-in condition is not contained within a single region. Instead, lock-in is *distributed* over several isolated regions along the entire length of the body, and is not limited only to the high current velocity region. However, despite this difference, the lock-in phenomenon remains a locally mono-frequency event, viz. vortex shedding occurs principally at a single frequency at a given spanwise location. This was first noted in the case of narrowband multi-frequency vibrations (Bourguet *et al.*, 2011*a*). In the

narrowband case, the lock-in condition is generally established at the locally predominant vibration frequency. For broadband responses, the spanwise evolution of the lock-in frequency is driven by the Strouhal relation.

The wake patterns are composed of spanwise cells of constant vortex shedding frequency that induce an oblique orientation of the vortex rows as they form, as well as vortex splittings between adjacent cells (Fig. 1). The vortex splittings are necessary to ensure the continuity of the vortex filaments while the vortex shedding frequency is discontinuous.

A comparison between the spanwise location of the lock-in region (Fig. 6(a)) and the in-line/cross-flow synchronization pattern (Fig. 5(a)) in the case of narrowband responses shows that the lock-in condition is preferentially established through counter-clockwise orbits, as also noted in a previous work (Bourguet *et al.*, 2011*c*).

The fluid force coefficient in phase with the cylinder velocity is used to quantify the energy transfer between the fluid and the structure (Newman & Karniadakis, 1997). A frequency decomposition of the force coefficient in phase with velocity including both the in-line and cross-flow contributions is plotted in Fig. 7 for each velocity profile. In these plots the predominant vibration frequencies are indicated by vertical dashed lines.

Positive energy transfer from the fluid to the structure, i.e. reinforcing structural vibration, occurs locally under the lock-in condition. As a consequence, the case of narrowband responses (Fig. 7(a)) exhibits a well-defined spanwise pattern composed of a zone of structure excitation located in the high current velocity area, and a zone of vibration damping located in the low current velocity side.

In contrast, several excitation and damping regions are alternating along the span in the case of broadband responses (Fig. 7(b)). It can be noted that these short regions of excitation, each with a different frequency and a spanwise extent which can be smaller than 5% of the cylinder length, lead to significant responses.

SUMMARY

The multi-frequency vortex-induced vibrations of a long tensioned beam in sheared current have been predicted by means of direct numerical simulation. Two profiles of oncoming flow velocity, a linearly varying profile and an exponentially varying profile, have been considered. In both cases the structural responses are mixtures of standing and traveling wave patterns. In the case of linear shear, the excited frequencies and spatial wavenumbers are concentrated within a narrow range, while broadband responses, involving both high and low structural wavenumbers, are identified in the exponential shear case.

The narrowband or broadband nature of the response impacts the spanwise pattern of wake-body synchronization. A single lock-in region is located on the high velocity side for the

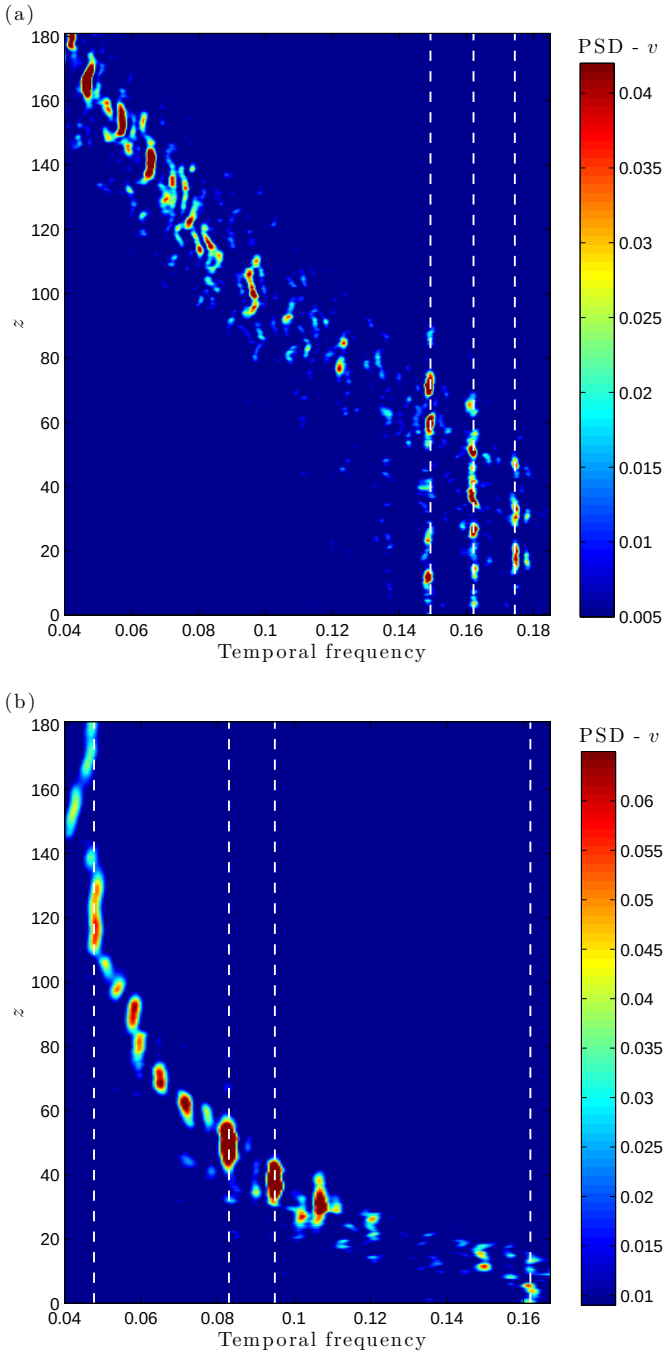

FIGURE 6. PSD OF THE TEMPORAL EVOLUTION OF CROSS-FLOW COMPONENT OF FLOW VELOCITY ALONG A SPANWISE LINE IN THE WAKE, IN THE CASES OF (a) LINEAR AND (b) EXPONENTIAL VELOCITY PROFILES. DASHED LINES INDICATE PREDOMINANT FREQUENCIES OF STRUCTURE VIBRATION.

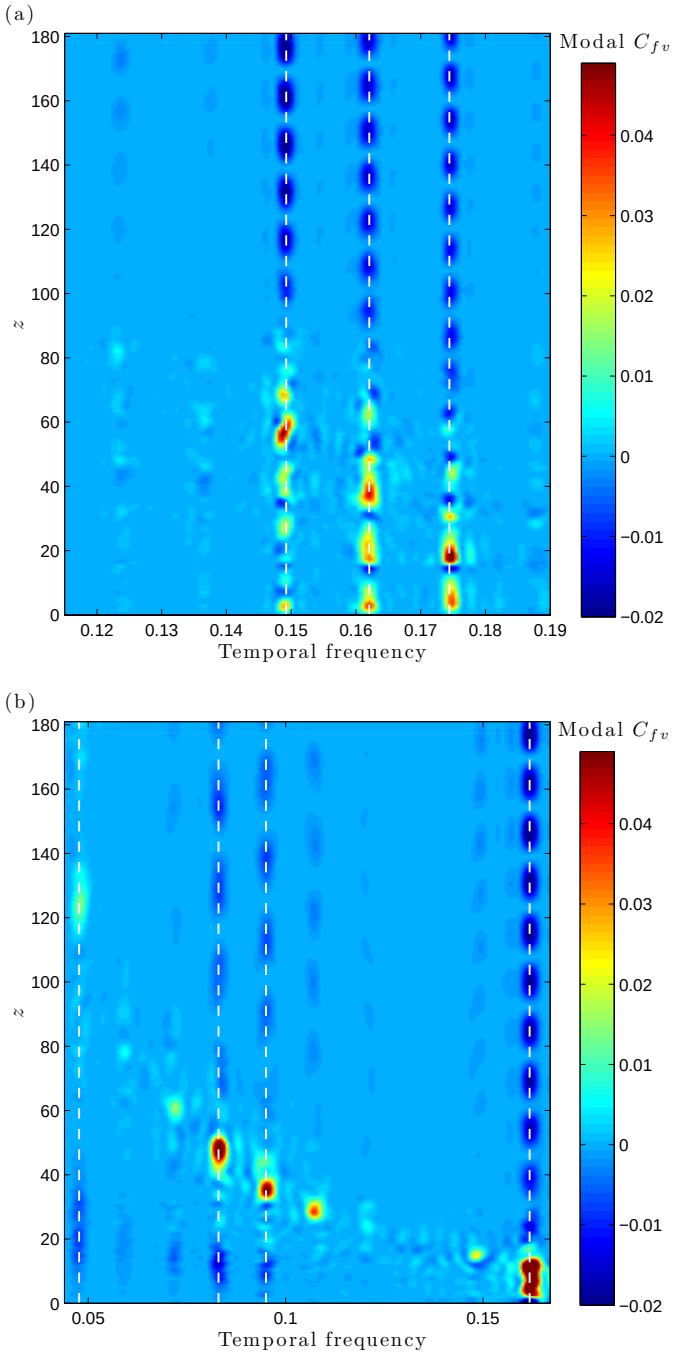

FIGURE 7. FREQUENCY DECOMPOSITION OF THE FORCE COEFFICIENT IN PHASE WITH THE CYLINDER VELOCITY FOR THE (a) LINEAR AND (b) EXPONENTIAL SHEAR CASES. DASHED LINES INDICATE PREDOMINANT FREQUENCIES OF STRUCTURE VIBRATION.

narrowband vibrations, while in the case of broadband responses the lock-in condition is distributed along the length of the body. The distribution of lock-in over several locations along the span brings changes to the synchronization between in-line and cross-flow responses: the phase drift between the two motions observed in the narrowband response is not observed for broadband response.

Hence, for narrowband response, a clear distinction between a single lock-in region contained within the high current velocity region, and a non-lock-in region over the rest of the span can be made. In the case of broadband response, alternating short regions of lock-in and non-lock-in are distributed over the span of the structure; each isolated lock-in region is characterized by a different frequency.

ACKNOWLEDGMENT

Financial support was provided by the BP-MIT Major Projects Program and BP America Production Co.

REFERENCES

Bearman, P. W. 1984 Vortex shedding from oscillating bluff bodies. *Annual Review of Fluid Mechanics* **16**, 195–222.

Bearman, P. W. 2011 Circular cylinder wakes and vortex-induced vibrations. *Journal of Fluids and Structures* Doi:10.1016/j.jfluidstructs.2011.03.021.

Bourguet, R., Karniadakis, G. E. & Triantafyllou, M. S. 2011*a* Vortex-induced vibrations of a long flexible cylinder in shear flow. *Journal of Fluid Mechanics* **677**, 342–382.

Bourguet, R., Lucor, D. & Triantafyllou, M. S. 2011*b* Mono- and multi-frequency vortex-induced vibrations of a long tensioned beam in shear flow. *Journal of Fluids and Structures* Doi:10.1016/j.jfluidstructs.2011.05.008.

Bourguet, R., Modarres-Sadeghi, Y., Karniadakis, G. E. & Triantafyllou, M. S. 2011*c* Wake-body resonance of long flexible structures is dominated by counter-clockwise orbits. *Physical Review Letters* **107**, 134502.

Carberry, J., Sheridan, J. & Rockwell, D. 2005 Controlled oscillations of a cylinder: forces and wake modes. *Journal of Fluid Mechanics* **538**, 31–69.

Chaplin, J. R., Bearman, P. W., Huera-Huarte, F. J. & Pattenden, R. J. 2005 Laboratory measurements of vortex-induced vibrations of a vertical tension riser in a stepped current. *Journal of Fluids and Structures* **21**, 3–24.

Dahl, J. M., Hover, F. S., Triantafyllou, M. S., Dong, S. & Karniadakis, G. E. 2007 Resonant vibrations of bluff bodies cause multivortex shedding and high frequency forces. *Physical review letter* **99**, 144503.

Evangelinos, C. & Karniadakis, G. E. 1999 Dynamics and flow structures in the turbulent wake of rigid and flexible cylin-

ders subject to vortex-induced vibrations. *Journal of Fluid Mechanics* **400**, 91–124.

Huera-Huarte, F. J. & Bearman, P. W. 2009 Wake structures and vortex-induced vibrations of a long flexible cylinder part 1: Dynamic response. *Journal of Fluids and Structures* **25**, 969–990.

Karniadakis, G. E. & Sherwin, S. 1999 *Spectral/hp Element Methods for CFD*. Oxford: Oxford University Press.

Lie, H. & Kaasen, K. E. 2006 Modal analysis of measurements from a large-scale viv model test of a riser in linearly sheared flow. *Journal of Fluids and Structures* **22**, 557–575.

Lucor, D., Mukundan, H. & Triantafyllou, M. S. 2006 Riser modal identification in CFD and full-scale experiments. *Journal of Fluids and Structures* **22**, 905–917.

Newman, D. J. & Karniadakis, G. E. 1997 A direct numerical simulation study of flow past a freely vibrating cable. *Journal of Fluid Mechanics* **344**, 95–136.

Ongoren, A. & Rockwell, D. 1988 Flow structure from an oscillating cylinder, part 1. mechanisms of phase shift and recovery in the near wake. *Journal of Fluid Mechanics* **191**, 197–223.

Prasanth, T. K. & Mittal, S. 2008 Vortex-induced vibrations of a circular cylinder at low reynolds numbers. *Journal of Fluid Mechanics* **594**, 463–491.

Sarpkaya, T. 2004 A critical review of the intrinsic nature of vortex-induced vibrations. *Journal of Fluids and Structures* **19**, 389–447.

Trim, A. D., Braaten, H., Lie, H. & Tognarelli, M. A. 2005 Experimental investigation of vortex-induced vibration of long marine risers. *Journal of Fluids and Structures* **21**, 335–361.

Vandiver, J. K., Jaiswal, V. & Jhingran, V. 2009 Insights on vortex-induced, traveling waves on long risers. *Journal of Fluids and Structures* **25**, 641–653.

Williamson, C. H. K. & Govardhan, R. 2004 Vortex-induced vibrations. *Annual Review of Fluid Mechanics* **36**, 413–455.